SUBJECT CATEGORIES FOR GODDARD JOURNAL

(To be used for classifying all NASA publications, journal articles, and other papers for inclusion in the Goddard Journal.)

Part A - Space Sciences

A 1. Astronomy and Astrophysics
A 2. Celestial Mechanics and Geodesy
A 3. Solar Physics
A 4. Ionosphere and Radio Physics
A 5. Fields and Particles
A 6. Planetology
A 7. Planetary Atmospheres
A 8. General (subjects not clearly belonging in any of categories 1-7)

Part B - Space Technology

B 1. Projects and Programs
B 2. Space Dynamics and Control Systems
B 3. Spacecraft and Subsystems
B 4. Vehicle Technology
B 5. Sounding Rockets
B 6. Sensors
B 7. General Electronics
B 8. Environmental Testing
B 9. Tracking Systems
B 10. General (subjects not clearly belonging in any of categories 1-9)

N 66-17 217

(ACCESSION NUMBER)   (THRU)

52

(PAGES)   (CODE)

TMX 56076

(NASA CR OR TMX OR AD NUMBER)   (CATEGORY)

FACILITY FORM 602

A VERTICAL TEST RANGE FOR ANTENNA RADIATION MEASUREMENTS

By

John Steckel and William Korvin

I. INTRODUCTION

In order to facilitate the measuring of satellite antenna radiation patterns under a controlled RF environment the concept of a "Vertical RF Test Range" was devised. The vertical test range configuration is shown in Figure 1.

Of primary importance was the test range's capability to adequately absorb and/or suppress undesirable electromagnetic energy as low as 125 Mc which would normally be reflected from the chamber walls and floor. The satellite antennas of concern are of the broad-pattern, near-omnidirectional type (i. e., dipole, turnstile, etc.).

The preliminary study, investigation, and 1/9-scale chamber model measurements indicated that a feasible reflection coefficient level of the order of 20 db to 25 db can be expected in an electrically small chamber of approximately $2\lambda \times 2\lambda \times 1\lambda$ in size. Subsequent full-scale measurements in the completed chamber have verified these reflection coefficient levels.

At higher frequencies of operation it was anticipated (and also indicated by 1/9-scale chamber model measurements) that the reflected energy level would be lower. The dominant controlling factor at higher frequencies is the structural weather protective radome. At the lower frequency the radome appears as a very thin wall (approximately 0.05λ thick). But as the frequency is increased, the presence of the radome becomes increasingly significant.
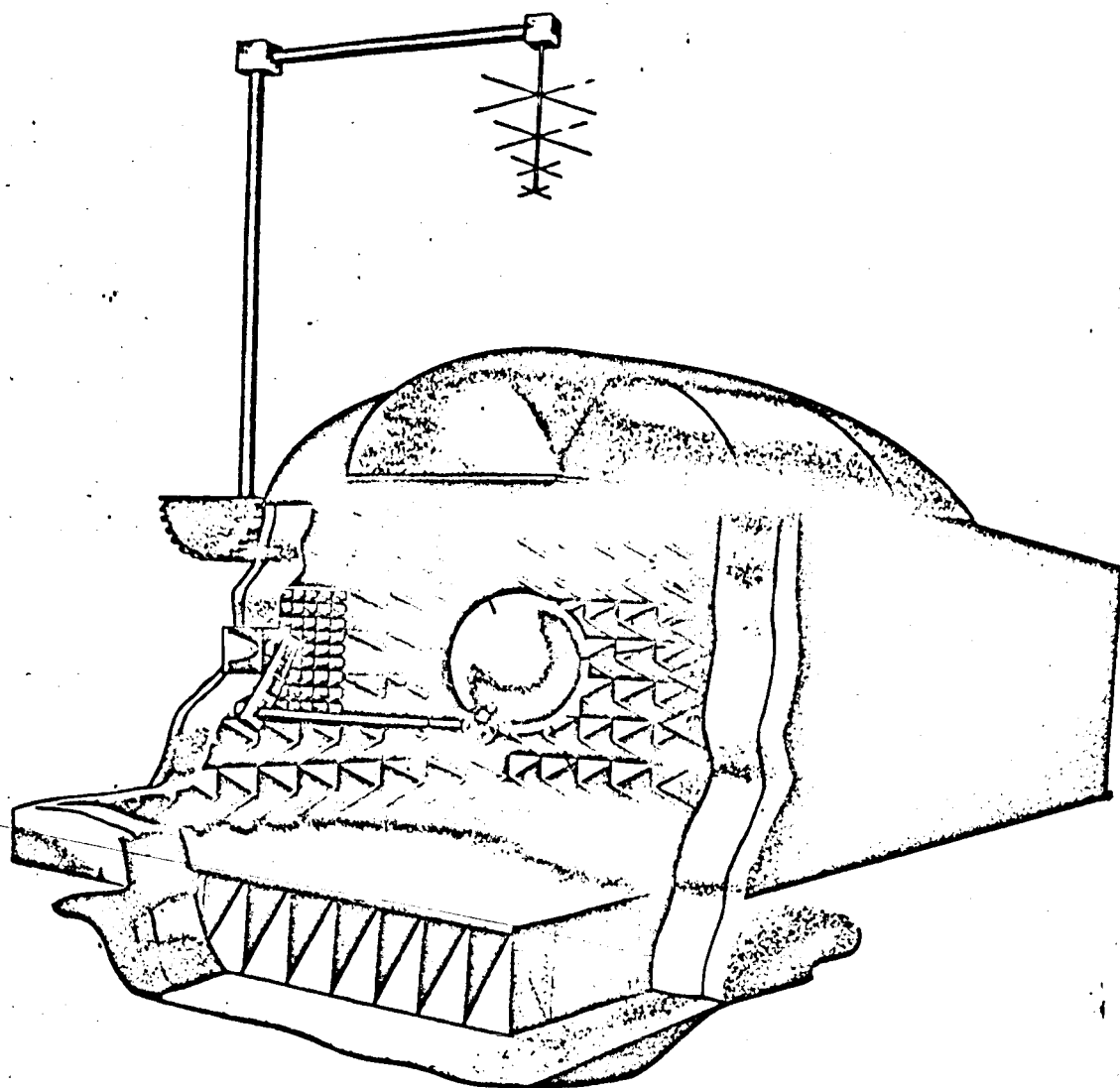
1

Figure 1-Vertical Anechoic Chamber

It should be remembered that an anechoic chamber is by no means free space. Therefore, it is of utmost importance that the RF anechoic chamber be "calibrated" not only as a function of frequency, but also as a function of illuminating or source antenna characteristics. Then, indeed, the confidence level at which the anechoic chamber may be used is defined.

II. Antenna Test Range Considerations

An antenna test range should be located in an area where parasitic reflections from objects in the vicinity are held to a minimum. In addition, the test range location should give consideration to possible active external radio interferences. Therefore, test range sites are normally located in relatively large cleared areas distant from extraneous radio signal sources. Special care must be taken when measurements are performed on small scientific spacecraft antenna systems operated in the UHF region and designed to be nearly omnidirectional in radiation pattern. This is a possible worst case condition for conventional antenna test range. Ideally we need an isolated reflectionless environment for these tests and a facility that will permit convenient operation. It is the recent advances in RF absorbent material and the proper use of these materials which has improved the performance of RF anechoic chambers to where they are comparable to the best outdoor range sites.

3

III. Definition of R-f Anechoic Chamber

A r-f anechoic chamber may be defined as an enclosure, suitably lined with an electromagnetic energy suppressing (ab-) sorbing and scattering) material, which may be used to measure such electrical characteristics as impedance, radiation pattern, and back scatter of a body within the chamber. Further, the degree of suppression of reflected undesirable electromagnetic energy shall be such as to approximate free space. The allowable divergence from free space is a function of the type of test and the tolerable error which the designer places on the test. For instance, a higher level of reflections may be tolerable when measuring impedance than when attempting back scattering measurements.

IV. Quality of a Chamber as a Function of Type of Test: Impedance, Back Scatter, and radiation Pattern

Measuring the impedance of an antenna system should be done ideally in the environment in which it is planned on being used. Unfortunately, many antenna systems are used in many environments. Therefore, the next best condition is to measure the system in "free space." This requirement at first thought appears extremely stringent, if not impossible. To meet the requirement explicitly would mean that an impedance measurement would have to be made at distances miles from the surface of the earth and from within the antenna system.

Fortunately, the requirement can be relaxed to a degree
governed by the tolerable error permitted in the system
impedance expressed as a Voltage Standing Wave Ratio.
Consider a perfectly matched antenna system radiating energy.
Under a condition of no electrical mismatch from external
sources there would be no standing wave and VSWR = 1.00:1.
In practice, all antenna systems exhibit some mismatch from
reflection resulting from electrical discontinuities. The
vector addition of the incident and reflected voltages results
in a standing wave, the magnitude of which is expressed in
the familiar form:

$$VSWR_{db} = 20 \log_{10} \frac{E_1}{E_2}$$

when

E_1 = incident voltage

E_2 = reflected voltage

This VSWR is an indication of the power transfer of an antenna system. For instance, a system with a VSWR of 6.0.1 would reflect 1/2 of the available power which is intolerable in most applications. Below is a brief table indicating the percentage of r-f power transmitted as a function of system VSWR.

VSWR	R-f Power Transmitted
1.00:1	100 %
1.04:1	99.6 %
1.22:1	99.02%

Since a perfect impedance match is seldom achieved the question then becomes how large a reflection due to the environment of the test site is tolerable while still permitting acceptable measurement of reasonable accuracy of the system impedance. Consider first, a worst case condition, i.e., all the incident energy striking a reflecting surface is reflected back to the antenna under test. If the power radiated P_0 from a perfectly matched antenna of unity gain, travels a distance R to a reflecting wall and is completely

reflected back to the antenna a standing wave will result. However, the inverse square law for the attenuation of electromagnetic energy will reduce the amplitude of the reflected wave such that the SWR induced will be less than infinite. For example, the attenuation of a 136 Mc signal to a reflecting wall 8 feet away can be computed from:

$$\alpha = 37 + 20 \log f + 20 \log R$$

where

α = attenuation (db)

f = frequency (mc)

R = distance (feet)

then

$$\alpha = 23.53 \text{ db}$$

Assuming perfect reflection from the wall, the signal will be further reduced by 6 db in the return path to the antenna. Thus, the returned signal will be about 29.5 db below the incident signal. The resulting mismatch to the perfectly matched antenna is computed from:

$$|\Gamma| = \frac{r - 1}{r + 1}$$

where

$|\Gamma|$ = reflection coefficient = 29.53 db
= .0335

∴ VSWR = r = 1.07:1

6

From the analysis above it is concluded that the impedance of a low gain antenna system may be measured with confidence if the walls of the enclosure are at least eight feet away and are less effective as a reflector than a metallic wall. Thus, the requirement on the absorption of unwanted reflections from the environment is easily met when making impedance or VSWR measurements on low gain antenna systems.

By definition, σ, the scattering cross section of a body is the ratio of the power scattered per unit solid angle to the power incident per unit area. In terms of the radar equation,

$$\sigma = \frac{P_R\ 16\pi^2 R^4}{P_T\ G_T G_R\ \lambda^2}\ \text{square meters,}$$

where

λ = the wavelength in meters.

R = the distance between the source antenna and the scattering cross section body in meters.

P_T = the transmitted RF power.

P_R = the received (reflected) RF power.

G_T = the transmitting antenna power gain with respect to an isotropic radiator.

G_R = the receiving antenna power gain with respect to isotropic radiator.

The problem which presents itself in measuring scattering cross sections in an anechoic chamber is the suppression of the energy from chamber

walls reflected back to a receiving antenna. The necessary chamber per-

formance, as in the case of VSWR measurements in a chamber, is relative.

For example, a large scattering cross section would reflect an energy level

which could be many orders of magnitude greater than energy contributed

by the reflected energy from the chamber walls (including ceiling). In this

case a percentage tolerance error can be established. Unfortunately, many

radar cross section measurements are made of objects which have a small

scattering cross section. Now, although the walls of the chamber absorb and

suppress the RF energy, the fact that the walls are many orders of magni-

tude in size larger than the object being measured results in a chamber wall

reflection coefficient which is as large as or larger than the object to be

measured. In other words, the scattering energy of the body to be measured

is hidden by the reflections from the chamber.

An example which illustrates the magnitude of energy suppression which

an anechoic chamber must exhibit for the measurement of radar cross

sections follows:

INSERT at A

TRANSMIT
&
RECEIVE ANTENNA

$R_1 \cong .9R_2$

$R_2 = 10$ meter

σ_1 σ_2

W

W

8
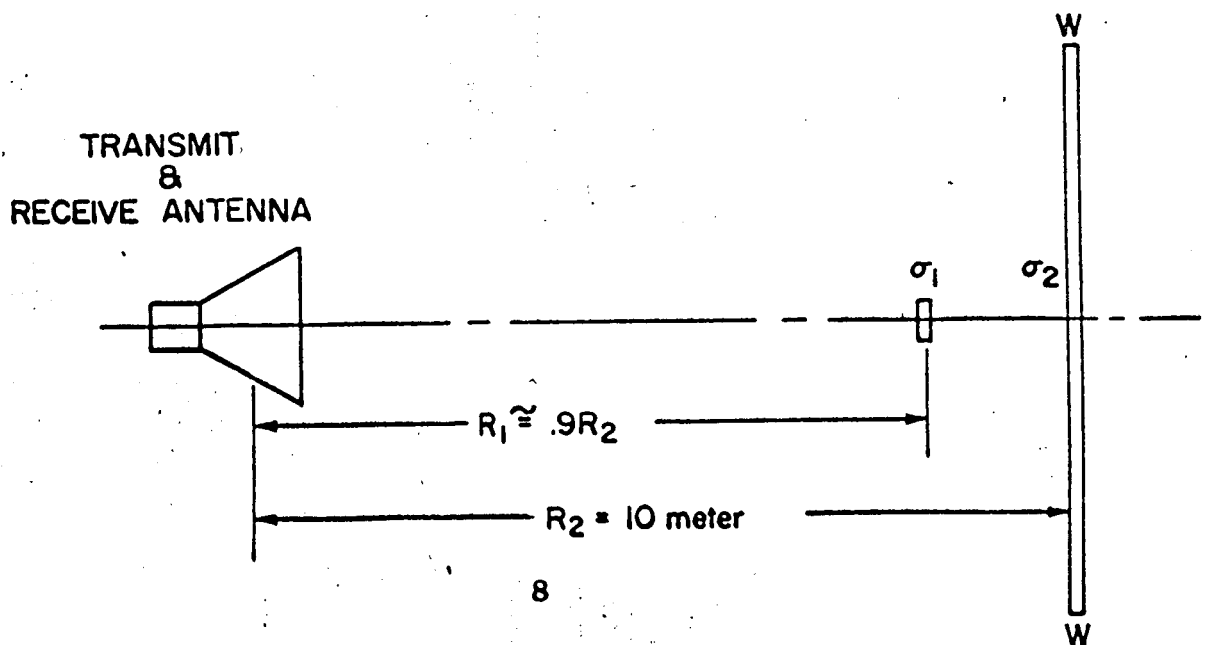
Let the scattering cross section be that produced by a sphere of radius $a = 0.1$ meter when the wavelength $\lambda = 3$cm (i.e., $a/\lambda > 1$). Then the scattering cross section $\sigma_1 = \pi a^2 = 3.14 \times 10^{-2}$ meter^2

Now, the return power received by an antenna G_r from a scattering body of cross section σ when the transmitted power P_T is radiated by an antenna G_T is,

$$P_R = \frac{P_T \, G_R \, G_T \, \lambda^2}{16\pi^2 \, R^4} \, \sigma$$

Consider first the return power received from the spherical scattering body and letting $P_T = 1$ watt, $R_1 = 9$ meters,

$$G_T = G_R = 63 \text{ and } \lambda = 3 \text{ cm.}$$

$$P_{R1} = \frac{P_T \, G_R \, G_T \, \lambda^2}{16\pi^2 \, R^4} \, \sigma_1$$

$$P_{R1} = .109 \times 10^{-6} \text{ watts}$$

Next, assume the wall w-w in the figure on page 8 to be a perfectly reflecting surface 3 meters on a side so that the wall radar cross section is

$$\sigma_2 \qquad \frac{4\pi \, A^2}{\lambda^2}$$

where A = area of wall and λ = wavelength at the operating frequency.
Then,

$$\sigma_2 \quad \frac{4\pi \, A^2}{\lambda^2}$$

9

$$\sigma_2 = 12.56 \times 10^4 \ M^2$$

The return power received from the back wall w-w is (the side, top and bottom walls may be neglected in this case since the predominant contribution to erroneous back scatter measurements is the back wall),

and, $P_{R_2} = .284$ watts

By comparison $P_{R_1}/P_{R_2} = -64.2$ db

Or, the energy normal to the back wall W-W must be suppressed by 64.2 db to allow the spherical body (.1 meter radius) to present an equal amplitude to the receiver antenna G_R. Of course, further suppression of the back wall energy must be attained before the energy from the spherical body is discernible from (i.e., above) the back wall scattered energy.

The example outlined above now allows a feeling for the nature and magnitude of energy suppression and/or absorbing characteristics that may be required of an RF anechoic chamber designed to measure radar cross sections.

Measurement of antenna radiation patterns generally requires a better anechoic chamber than one for the measurement of antenna impedance. But the requirements are not as critical as for radar cross section (back scatter) measurements.

As an illustration, let us examine a typical E-plane pattern of a horn antenna and then show the effects of various magnitudes of reflected energy interfering at various aspect angles in the chamber. Figure 2 shows the

E-plane pattern as measured in a controlled environment at an outside antenna range. The pattern approaches the theoretical pattern for a horn antenna exhibiting uniform distribution across the aperture. Figure 2 also shows a ray outline of reflected energy when measuring the E-plane pattern of this antenna in an anechoic chamber. Let sources of reflection be located at angles defined by $\theta = 50°$ and $60°$. Then the resulting perturbations from these reflecting sources are shown in Figure 2 as dashed lines. The deviations in the pattern are identified as ①, ②, and ③. The magnitude of the perturbation at ① is 1.6 db. The magnitude of the reflected energy from point I which produces this 1.6 db is equal to 21 db since the reflection coefficient in db = 20 log (S - 1/S + 1), where S = standing wave ratio. Refering to the figure, it can be seen that the perturbations take place at -14.2 db on the radiation pattern. Therefore, the actual reflection coefficient (magnitude of the interfering reflected energy) is equal to 35.2 db. At point ② the deviation from point II is 1.1 db or a reflection coefficient of 25 db. Since the radiated energy is down 15.5 db at this point, the actual reflection coefficient is 40.5 db. Now consider point ③ (i.e., 0 db down on the pattern). A refection coefficient of 40 db will cause a 0.175 perturbation in the pattern at this point.

From the above exercise one can now see clearly the effect of reflected energy on a typical pattern from arbitrarily chosen points in an anechoic chamber enclosure which is 35 db to 40 db down from the incident energy.
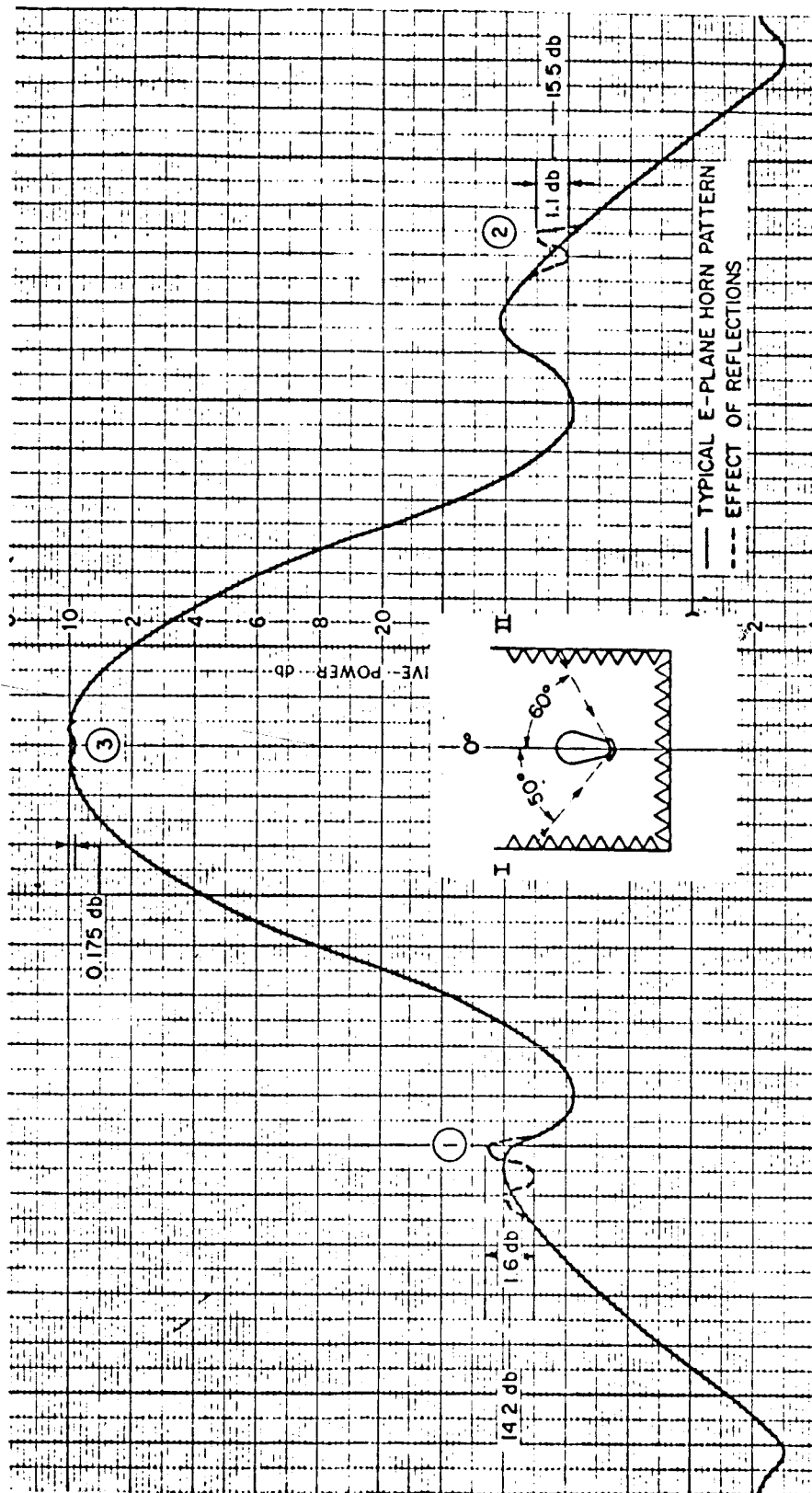
Figure 2-Effect of Reflected Energy on Typical E-Plane Pattern of Horn Antenna

V. Vertical RF Test Range Description

The vertical test range is as shown in Figure 1. The walls and floor of the structure are reinforced concrete. Attached to the chamber through a common wall is the control room which houses all the electrical measuring devices. Opposite the control room side are two doors which when opened allow the chamber to be used as one end of a horizontal antenna range in conjunction with available antenna towers. The roof of the chamber is an A-sandwich type RF transparent radome. Also, shown in this figure is the ~~outside azimuth - elevation mount and fiberglas mast approximately 35 feet above the chamber controlled from inside.~~ *controlled from inside, that holds a fiberglass mast assembly that positions an antenna approximately 35 feet above the test model.* This facilitates the changing of source antennas. Inside the chamber (see Figure 3) is a wall-mounted antenna mount capable of rotating and allowing measurement of a satellite antenna system at or near the center of the chamber quiet zone.

The walls are lined with pyramidal absorbent material 70 inches in length on 2 feet square bases (Figure 4). In the area of the side wall mount smaller pyramidal absorbent material is used allowing the rotation of an off-set arm containing the fiberglas mast. The floor of the chamber is lined with foam structure 70 inch pyramids on top of which is cemented a smooth floor - decking material of 1/2" thick sheets of semi-rigid vinyl foam which can be walked upon in setting up experiments within the chamber.
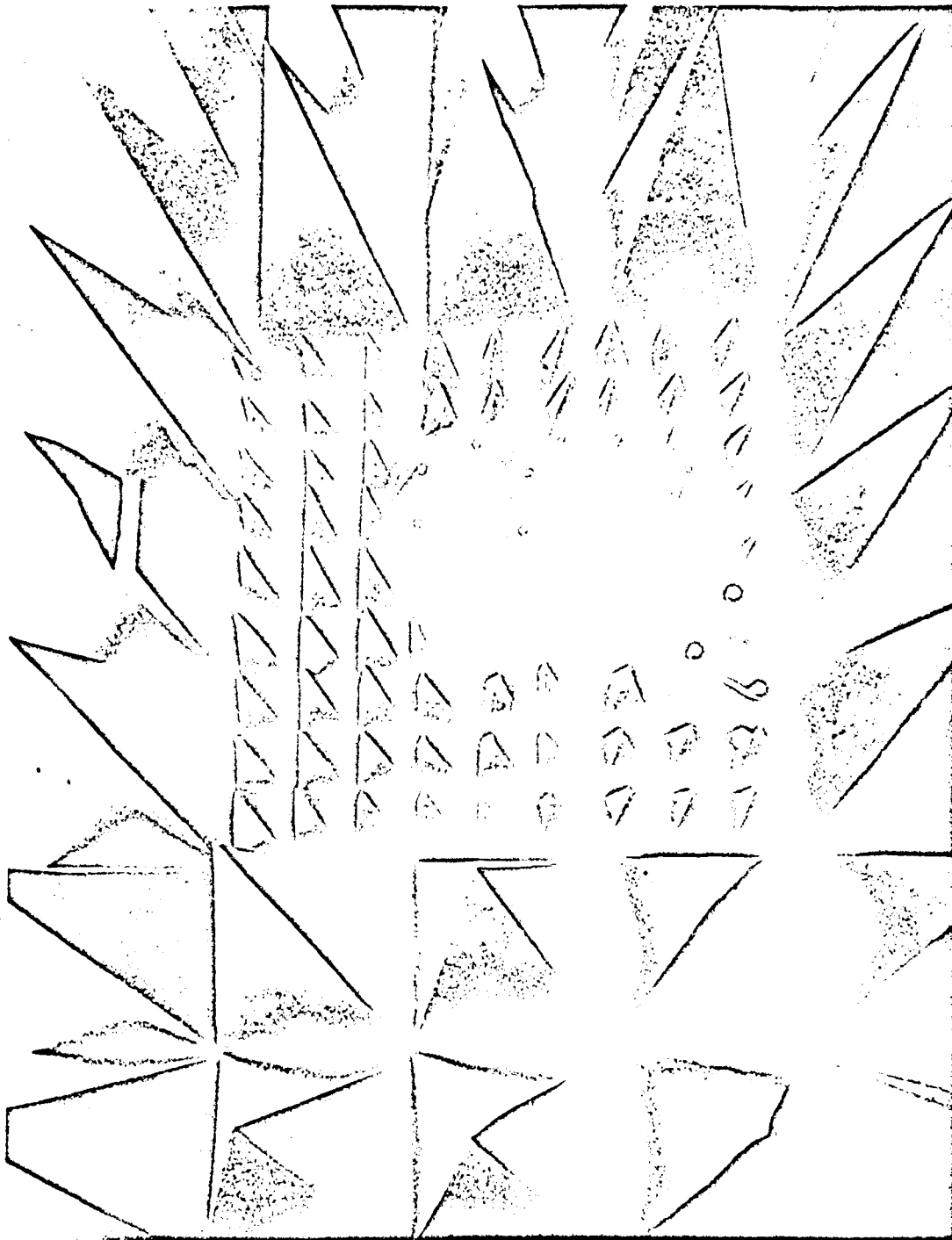
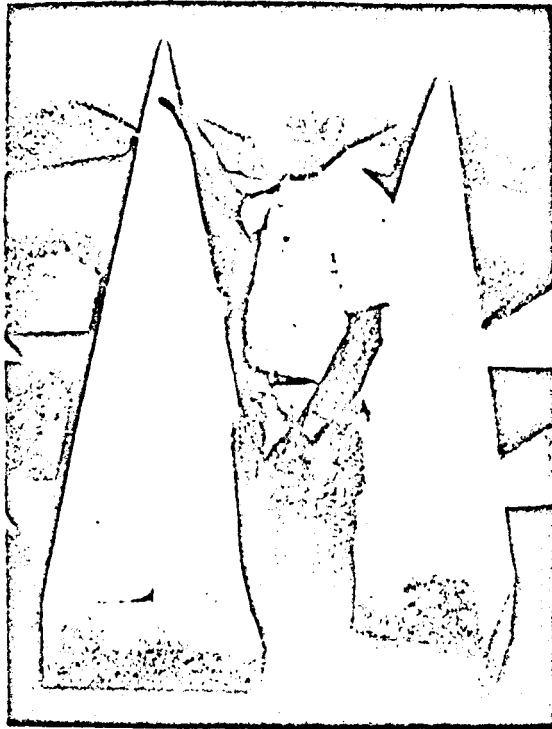Figure 3.-Photograph of Wall Mount Inside Chamber

Figure 4-Photograph Illustrating Size
of Absorbent Material

The radome is a structural body of the A-sandwich type. It is approximately 4" thick and the 9 sub-pieces are assembled into a continuous weather protective roof (Figure 5).

Uniform chamber lighting is achieved by directing four flood lamps toward the radome. The four lamps are located at the four upper corners of the chamber such that they are well hidden by the absorber on the walls. This technique of lighting results in two very favorable conditions; the lighting is uniform and avoids the visual problem of looking into the lamps; a minimum of RF reflection from the fixtures is obtained since they are well shadowed by the 70" absorbent material.

Finally, the chamber is temperature controlled to prevent large variations of temperature which may effect antenna measurements.

Electrically the chamber was lined on 5 surfaces with an RF absorbent material and the 6th side enclosed by an RF transparent (radome) roof. Each individual piece of the material is a 70" high pyramid shaped absorber on a 2 feet square base. All of the absorbent material exhibits a minimum reflection coefficient of 28 db at 120Mc, 40db at 400Mc and 50db at 1,000 to 10,000 Mc.
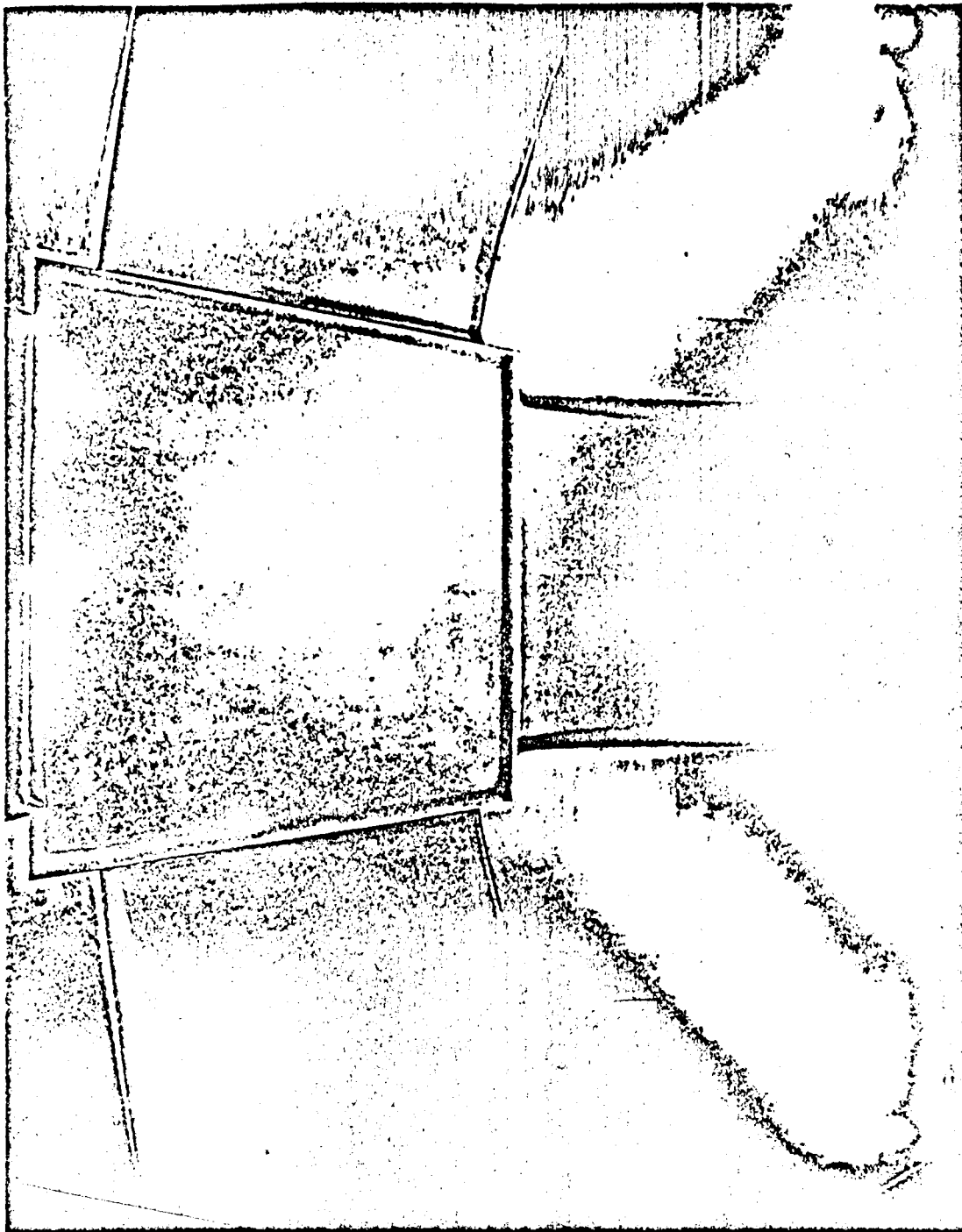
Figure 5-Photograph of 9 Panel Radome

The tests on the absorber at the manufacturer's plant were made in a closed loop technique at 120Mc and 400Mc. At 1,000, 5,000 and 10,000Mc an open loop technique was used. The closed loop technique consisted of measuring four 2'X2' absorber pieces at a time in a flared waveguide system in which the absorbent material serves as a load under test. The absorber is moved inside the waveguide resulting in a standing wave that moves in conjunction with the physical movement of the absorber. A fixed probe inside the waveguide located between the absorber and RF oscillator detects the standing wave which is converted to power reflected.

The open loop technique of testing consisted of a horizontal version of the NRL type arch method. A reference was used which consisted of a flat 2'X8' metal plate. The reflection level of four 2X2 pieces was measured and compared to the flat metal plate. The reflectivity of the absorbent material is the difference in return power in db between the metal plate and the absorbent material.

The electrical characteristics of the A-sandwich radome material were specified as:

(a) Transmission loss $\leqslant$ 7.5% over the frequency range of 120Mc to 10,000Mc.

(b) Refraction less than 10% for angles of incidence from 0° to 45°.

(c) Loss tangent of glass laminate = .005.

(d) Dielectric constant of glass laminate = 4.0.

(e) Loss tangent of foam core = .0005.

(f) Dielectric constant of foam core = 1.12.

Although tests at the manufacturer's plant confirm the meeting of the specifications on a flat 40"×40" sample of the radome, measurements indicate that the actual radome does exhibit less than specified performance particularly at frequencies above 1,000Mc. This can be easily explained since the actual completed radome possesses a curved surface and the nine pieces comprising the total radome are assembled with beefed-up glass laminate flange sections. These two conditions increase the detrimental effects (increased diffraction and reflection).

As previously stated the frequencies of primary interest are in the 120Mc to 400Mc region. But some tests were performed in the chamber at higher frequencies.

Normally, in evaluating the chamber a quiet zone is defined. That is, a volume within the chamber in which known (measured) reflectivity levels exist. Then in this zone antenna systems can be evaluated being fully aware of the limitation of the chamber. Therefore, by definition, the quiet zone *in this chamber* is a 10 foot diameter sphere which is tangent to the chamber floor and centered elsewhere within this chamber.

VI. Advantages of Vertical Test Range

Ground reflections are the most serious source of error when using a conventional test range for measurements of low frequency, low-gain antennas. The error may be reduced to a degree by additional height to the towers, but towers over 100' high are expensive and rather inconvenient to use. Likewise a conventional anechoic chamber designed for operation at low frequency is expensive and requires a large building to provide even a modest size test range. The vertical test range provides an attractive compromise between tall towers and a large anechoic chamber. The chamber portion need only be large enough to prevent reflections from the ground and nearly reflecting surfaces and the tower need only be tall enought to hold an antenna out of the near field of the antenna under test. Furthermore, the length of the test range may easily be varied by adjusting the height of the outside antenna. Operation of a vertical range is especially convenient. The model under test, the test and control equipment, and personnel are all at ground level and thus avoid the need for hoists and elevators. Also, the antenna system under test is not subject to rapid change in weather, inclement weather or high wind velocities.

VII. Vertical Test Range Chamber Analysis

The magnitude of unwanted reflections that can be tolerated in an antenna test range have been shown to be a function of the parameter being measured. Since the site is never perfect, the results obtained may be interpreted in terms of the known site imperfections provided the reflection coefficients and in some cases phase are accurately specified. However,

measurement of reflection co-
efficient of absorbent material is difficult and techniques for its evaluation have

not been standardized. Currently the Pattern Comparison Technique[1] and the

Free Space VSWR Technique[2] are favored in evaluation of r-f anechoic chambers.

In both techniques the significant result is the comparison of the incident to the

reflected energy from an absorbing wall to determine its reflection coefficient.

Briefly, in the Pattern Comparison Technique, the pattern of a directive

antenna (15 to 20 db gain) is measured successively at closely spaced points

along the radii of the chamber quiet zone. ~~The quiet zone may be defined as the~~ *out?*
~~volume within an anechoic chamber in which an antenna under test will be meas-~~
~~ured.~~ Then the patterns are superimposed on each other with pattern peaks

coincident. The deviations in the patterns are read at different aspect angles

and VSWR curves vs aspect angle are constructed. The curves may then be con-

verted to reflection levels within the chamber.

The Free Space VSWR Technique is a method of continuously recording the

amplitude variations produced by reflections. Two directive antennas are used,

with one being moved continuously across the chamber quiet zone at a discrete

aspect angle for each recording. The amplitudes recorded are reduced to inci-

dent and reflected energy levels, thus allowing the reflection coefficient vs aspect

angle of a chamber to be determined.

From the brief summary above (and more so from the referenced literature)

it can be seen that both techniques rely on use directive antennas. This is not

a disadvantage in the usual situation where the chamber is large in terms of wavelength and directive antennas are usually evaluated. However, in the vertical test range more emphasis is placed on measurement of nearly omni-directional antennas in a termination chamber that is electrically small, i.e., approximately 1λ in depth and 2λ on a side. Although evaluation of chamber performance using directive antennas will indicate both a direction and reflection coefficient for sources of reflections, unless considerable effort is made to integrate the reflection levels from all directions the chamber will appear better than when used with an omnidirectional antenna. Therefore most of the analysis of both the scale model and the full scale range was made using a dipole antenna to probe the energy levels within the termination chamber. In this method, a dipole antenna is moved throughout the quiet zone and energy levels vs position recorded. The difference between the levels recorded and calculated free space levels are converted into VSWR and finally a reflection coefficient computed.

It is common practice to try to reduce the large number of different reflection coefficients that are measured in evaluating a chamber to a single number that is then used to define the chamber's performance. In general, it will be found that this number is not really a common denominator and that the relative perform-ance of two different chambers should not be judged on this alone. For instance the quiet zone of chamber A may be only 1/3 the volume that was included in evaluation of chamber B, yet chamber B may be considerably better than A over

the same quiet zone. Unfortunately, the performance rating
of anechoic chambers is like the evaluation of radio receivers
in 1940, i.e., not complete unless the test conditions are
known as well as the results.

VIII. <u>Preliminary Investigation-1/9th Scaled Chamber</u>
<u>Measurements</u>

A preliminary investigation of the characteristics
of an electrically small anechoic chamber was performed using
a 1/9th scaled chamber (figure 6). The scaling technique
approach was used to determine the order of magnitude of
reflection coefficient which could be expected in the full
scale chamber. No attempt was made to design and test a
scaled radome because the radome appears as a thin wall
structure (i.e., less than $\lambda/8$) at the frequencies of interest
(up to 400 Mc) in the full scale chamber Figure 7 shows the
test set-up for the 1/9th scaled measurements.

• Although no scaled radome measurements were made in this
instance some general comments on scaled radome measurements
are in order. In general scaling a multi-panel, sandwich
radome is difficult. The scaling of radome interval ribbing,
panel flanges and radome curvature must be handled with extreme
care. Serious errors can be expected if this precaution is
not taken. Radomes of the thin wall class with dielectric
constants of approximately 3 or 4 and also thick wall foam
radomes of low dielectric constant ($\epsilon \approx$ 1.1 to 1.4) are practical
for scaling purposes.

Frequencies from near 1,080Mc to 3600Mc were used in measuring the characteristics of the 1/9 scaled model (corresponding to approximately 120 Mc and 400Mc respectively full scale). A dipole antenna is used to probe the chamber to deliberately prevent discrimination against any reflected energy. Directional antennas would have been too selective.

At 1080Mc in the 1/9th scaled chamber the reflection coefficient measured was about 20db and at 3600Mc the reflection coefficient was 30 db.

Standing waves typical of these measurements by probing the scaled chamber are shown in figure 8. The dipole probes were moved in small increments in terms of wavelength from the aperture of the chamber to the back. The curves of figure 9 depict standing waves resulting from probing across the chamber in small increments. This data is typical of that obtained from the 1/9th scaled chamber. It was from these scaled measurements that the performance of a full scaled chamber was predicted.

IX. Full Scale Chamber Measurements

The quiet zone of the chamber was probed with a dipole using an overhead illuminating antenna which was directional in nature.
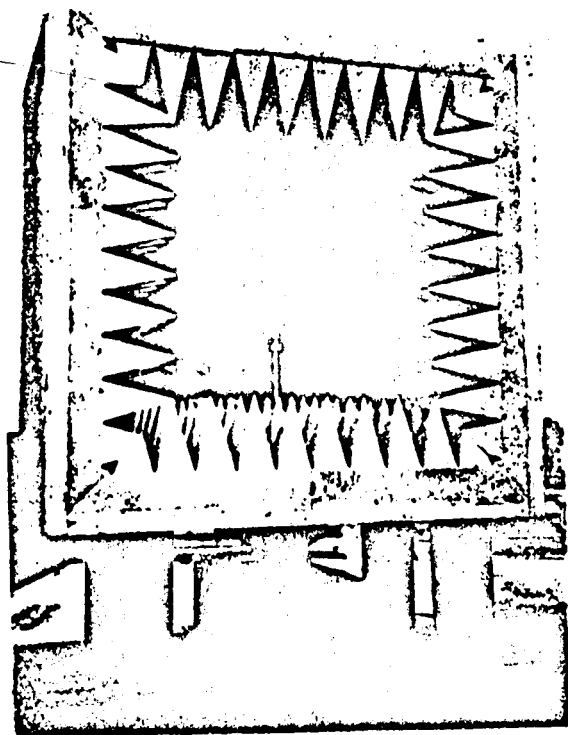
Figure 6–Photograph of 1/9th Scale Chamber
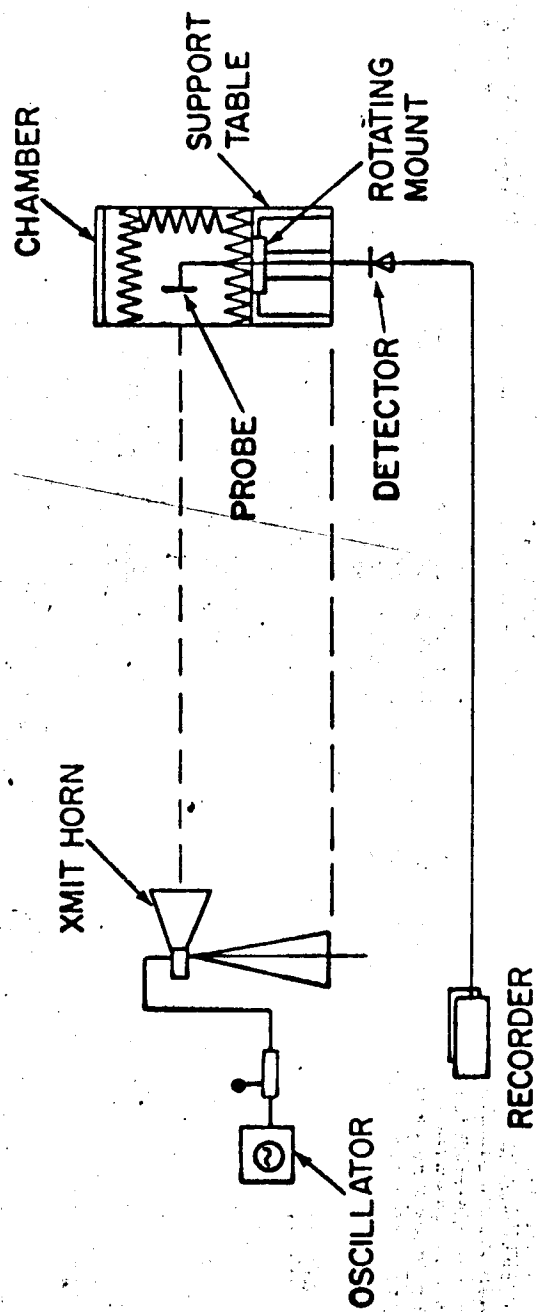
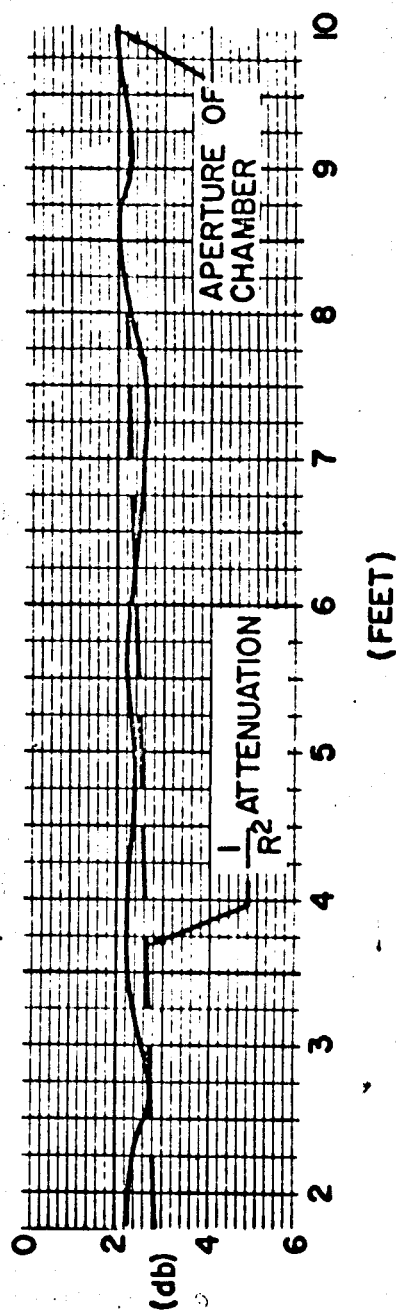Figure 7—Equipment Set-Up for 1/9th Scale Measurements

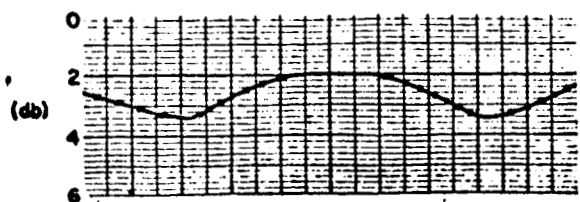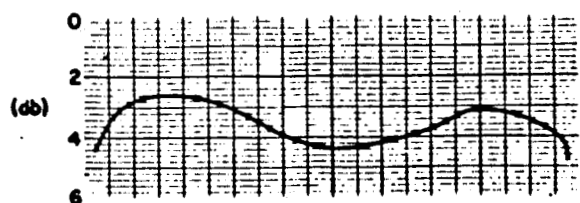Figure 8—Standing Waves in 1/9th Scale Chamber Measured from Aperture of Chamber Floor

27

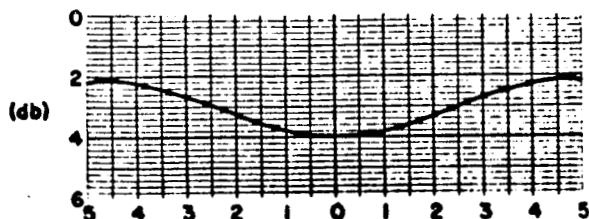I/9 SCALE CHAMBER
f = 1080 mc
DIPOLE PROBE
S/A HORN

I/9 TH SCALE CHAMBER
f = 3600 mc
S/A GAIN STANDARD
DIPOLE PROBE

(db)

POSITION NO.I
REFL. COEFF ~ 21 db

POSITION NO.I
REFL. COEFF ~ 31 db

(db)

POSITION NO. 2
REFL. COEFF ~ 21 db

POSITION NO.2
REFL. COEFF ~ 32 db

(db)

POSITION NO.3
REFL. COEFF ~ 21 db

POSITION NO.3
REFL. COEFF ~ 32 db

PROBE
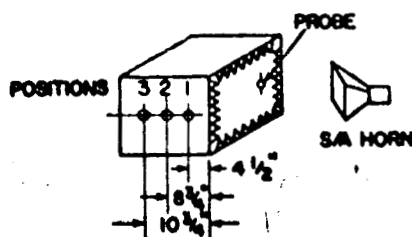
POSITIONS

S/A HORN

4 ½"

8¼"

10⅞"
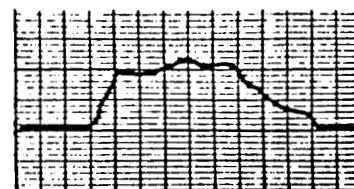
Figure 9-Standing Wave Curves Measured Across 1/9th Scale Chamber Aperture

28

Specifically, at 125Mc and 400Mc the magnitude of the reflection coefficient was determined by moving a dipole horizontally inside the chamber in directions normal to each wall and across the diagonals. With the dipole fixed to a cart made of low dielectric constant foam material, the cart was moved along tracks which could be oriented as desired within the chamber. The track, cart and dipole support are shown in Figure 10. There horizontal measurements were made at discrete heights of 2 (and/or 3), 4, 5, 6 and 8 feet above the floor of the chamber. The reflection coefficient in the vertical direction was determined by measuring the standing wave as a function of vertical movement of the dipole from 2 to 10 feet above the floor. Resulting standing wave curves are converted to an equivalent reflected energy level (reflection coefficient). Figure 11 is a typical curve. The dashed curve of Figure 11(b) represents the probed energy level as measured in Figure 11(a) in the absence of reflected energy. The solid curve superimposed on the dashed curve represents the effect of the reflected energy. Peak to peak value of the standing wave is 0.5 db. This standing wave of 0.5 db results from a reflected energy level of 30 db below the incident signal level. Or, Reflection Coefficient = 20 log VSWR-1/VSWR+1. Measured curves are shown in Figures 12(a) through 12(d).

At 1,200Mc reflected energy levels greater than expected were measured (approximately 32 db average). Also, the reflected energy levels were polarization sensitive (i.e., E-perpendicular vs E-parallel) with differences in
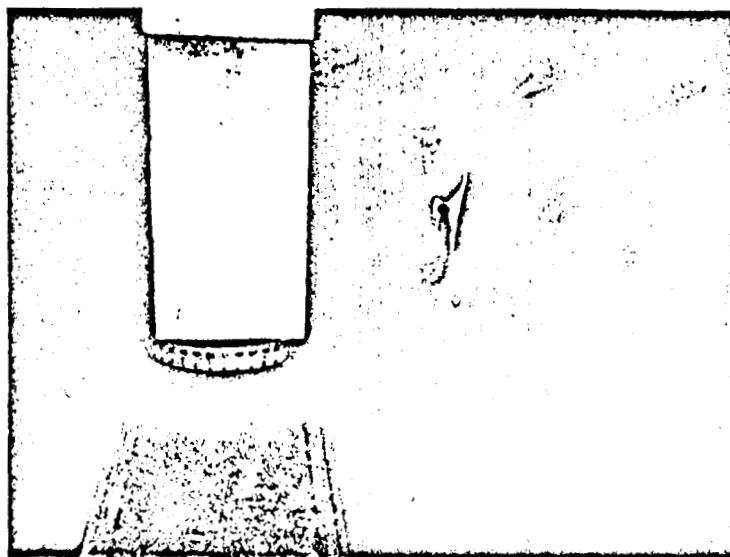
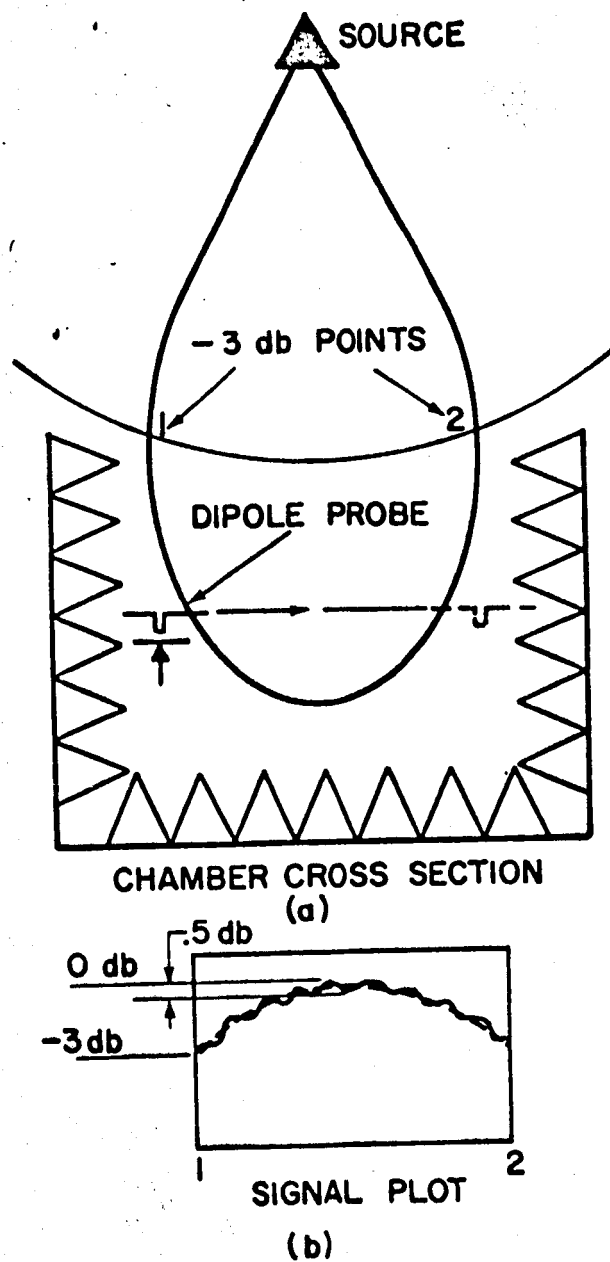Figure 10—Photograph of Track and Cart Arrangement

SOURCE

−3 db POINTS

1   2

DIPOLE PROBE

CHAMBER CROSS SECTION
(a)

.5 db
0 db
−3 db

1   2
SIGNAL PLOT
(b)

Figure 11–Interpretation of Standing Wave Curves

VERTICAL MEASUREMENT (FULL SCALE)

$f = 125$ mc

$\theta = 0°$

REFL. COEFF ~ 22 db

APERTURE OF CHAMBER

$\dfrac{1}{R^2}$

1.3 db
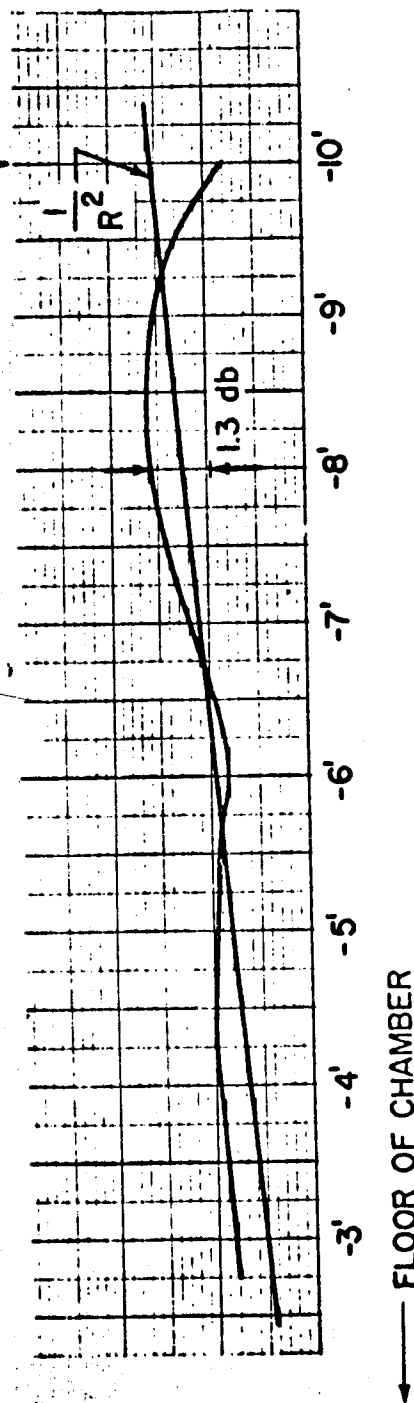
-10' -9' -8' -7' -6' -5' -4' -3'

FLOOR OF CHAMBER

Figure 12a—Full Scale Chamber Standing Waves at 125 Mc, 400 Mc

32
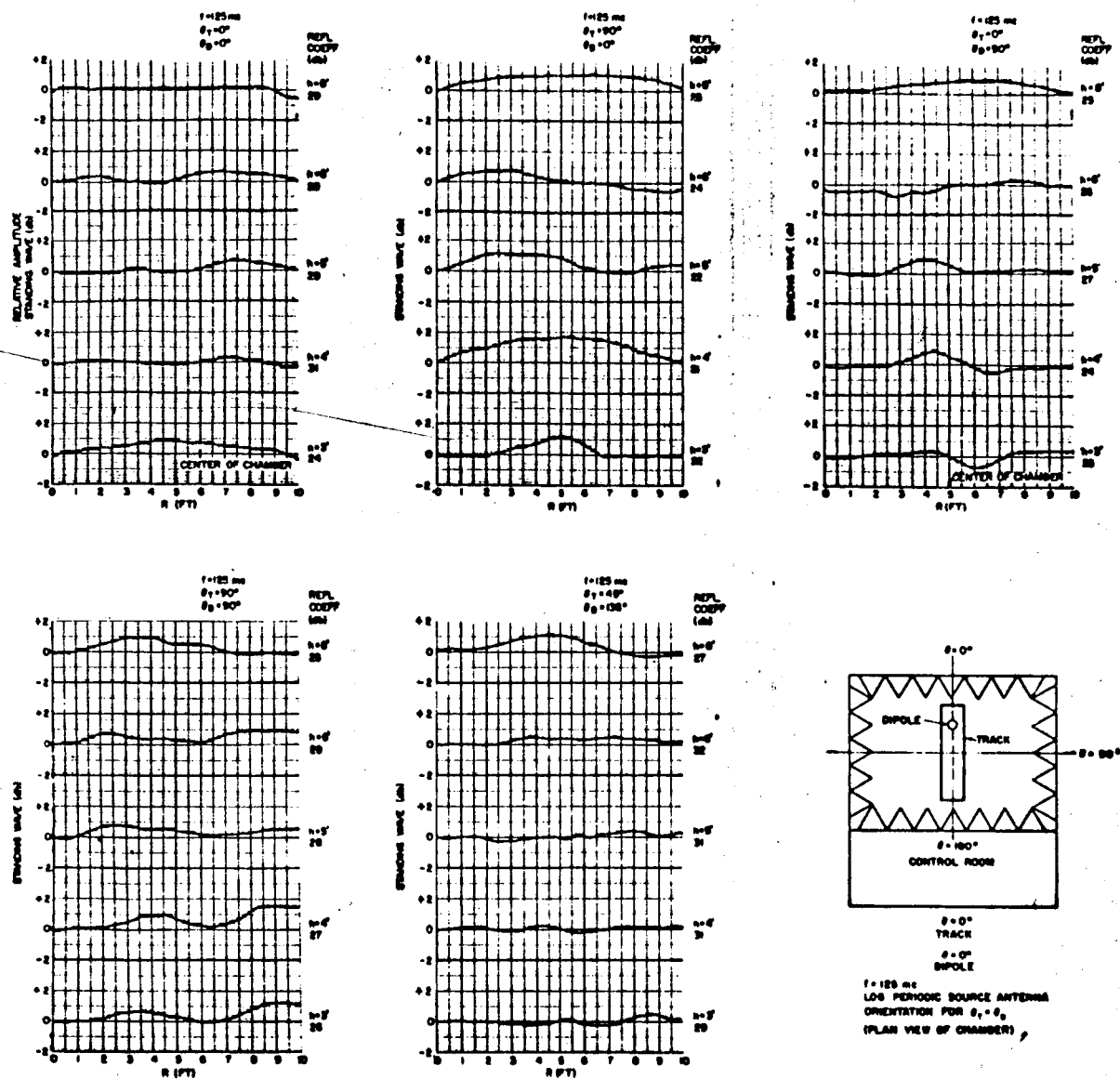
Figure 12b—Full Scale Chamber Standing Waves at 125 Mc, 400 Mc

VERTICAL TEST
θ = 0°
f = 400 mc
REFL. COEFF ~ 31 db

FLOOR OF CHAMBER

R =

h=2'   h=3'   h=4'   h=5'   h=6'   h=7'   h=8'   h=9'   h=10'
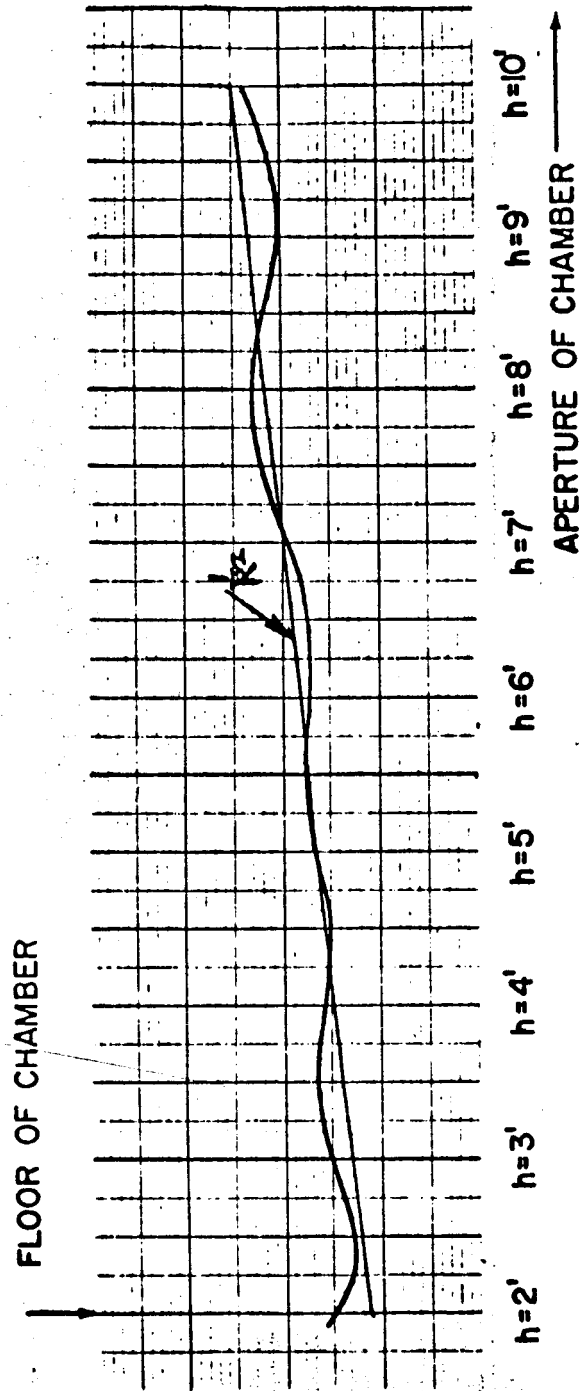
APERTURE OF CHAMBER

Figure 12c.–Full Scale Chamber Standing Waves at 125 Mc, 400 Mc
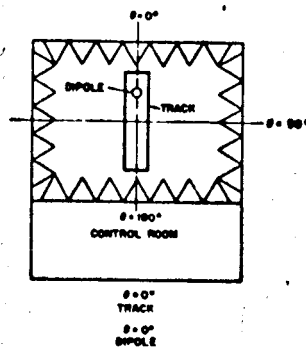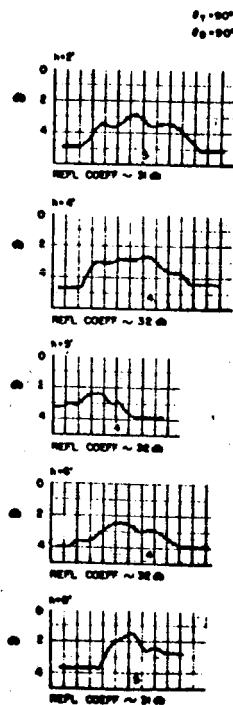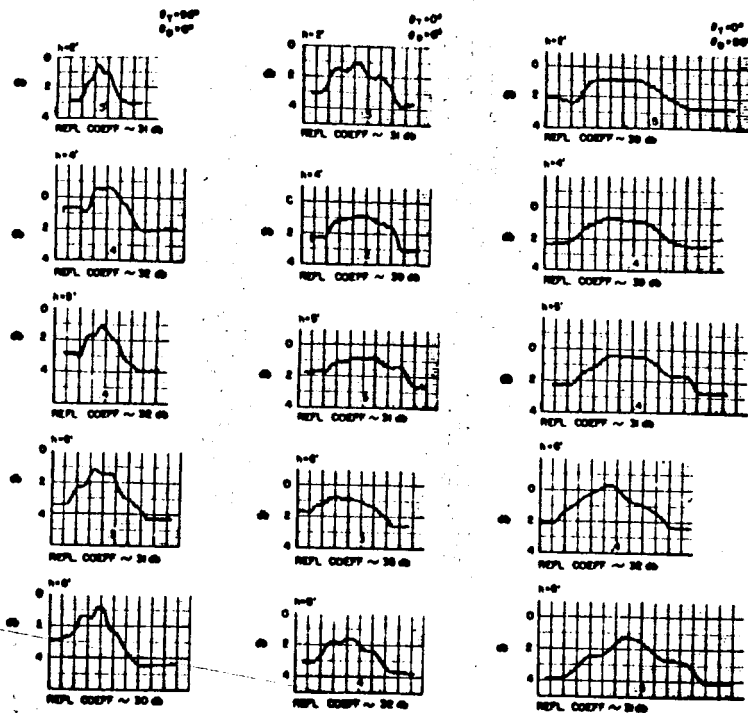
34

Figure 12d–Full Scale Chamber Standing
Waves at 125 Mc, 400 Mc

reflection coefficients between 6 and 15 db as a function of aspect angle. This obvious deviation from the 45 to 50 db levels anticipated was attributed to the radome for two reasons:

(1) The chamber at 1,200Mc is electrically large ($15\lambda \times 15\lambda \, 10\lambda$) and therefore the chamber would be expected to be much better than at 400Mc (reflection levels $\approx$32 db).

(2) This A-sandwich radome (4 inches thick, with solid fiberglas panel flanges) appears as a relatively large discontinuity.

Measured magnitudes of reflected energy for various linear polarization orientations when probing the chamber at 125Mc and 400Mc are tabulated in Tables 1 and 2. Some inconsistency is apparent, especially in the higher coefficient values measured at 125Mc. This is attributed to instability of the measurement equipment; however, retests of selected orientations indicate no serious differences from the data presented or the conclusions drawn from the data.

Table 1

125Mc Chamber Reflectivity Levels

Track Orientation θ_T	Dipole Orientation θ_D	Dipole Height Above Floor				
		3 ft.	4 ft.	5 ft.	6 ft.	8 ft.
0°	0°	24 db	31 db	29 db	29 db	29 db
0°	90°	25 db	24 db	27 db	26 db	25 db
90°	0°	*27 db	*26 db	*28 db	*24 db	*20 db
90°	90°	26 db	27 db	28 db	29 db	25 db
45°	45°	29 db	22 db	24 db	23 db	*25 db
45°	135°	29 db	31 db	31 db	32 db	27 db
135°	45°	26 db	21 db	21 db	21 db	22 db
135°	135°	*22 db	*21 db	*24 db	*24 db	*21 db

*Measurements performed at 123Mc using NASA
battery operated signal generator.

Table 2

400Mc Chamber Reflectivity Levels

Track Orientation θ_T	Dipole Orientation θ_D	Dipole Heights Above Floor				
		2 ft.	4 ft.	5 ft.	6 ft.	8 ft.
0°	0°	31 db	39 db	31 db	35 db	32 db
0°	90°	39 db	39 db	31 db	32 db	31 db
90°	0°	31 db	32 db	32 db	31 db	30 db
90°	90°	31 db	32 db	32 db	32 db	31 db
45°	45°	31 db	39 db	39 db	34 db	32 db
45°	135°	32 db	31 db	30 db	31 db	32 db
135°	45°	35 db	32 db	31 db	35 db	30 db
135°	135°	32 db	32 db	30 db	31 db	39 db

Data taken at 1,200Mc are not presented because later tests prove that the radome is the major contributor to standing waves within the chamber and therefore does not truly represent the capability of a vertical test range.

To verify the fact that the radome was the major contributor to the problem (i.e., larger reflection coefficients than anticipated and polarization sensitivity) measurements were performed with the source antenna inside the chamber just under the radome and compared to the pattern taken through the radome. Thus, an interference pattern between incident and reflected energy was produced by essentially removing the radome from between the source and receive antenna. In both cases a horn antenna was moved across the chamber.

The two polarization conditions E-perpendicular and E-parallel are defined below.
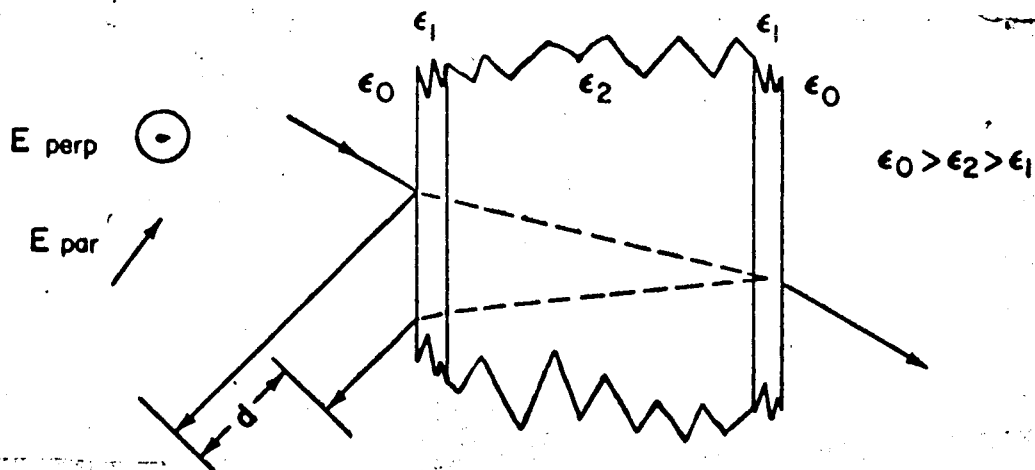
Except at angles far off normal incidence reflected
energy from E-perpendicular is nearly always greater than
E-parallel because of the zero at the Brewster angle occuring
only with parallel polarization. The Brewster angle (where
the reflection value goes to zero) is defined as follows:

$$\theta_B = \tan^{-1}\sqrt{\frac{\epsilon_2}{\epsilon_1}} \quad \text{when } \epsilon_2 > \epsilon_1$$

$$\theta_B = \tan^{-1}\sqrt{\frac{E_2}{E_1}} \quad \text{where } E_2 > E_1$$

An important point which is illustrated in Figure ~~15(a)~~ 13(a),
(b) is the degree of accuracy with which the antenna radiation
patterns can be measured through a radome which exhibits
significant reflection characteristics. In this case the
radiation patterns of an antenna (gain standard at 1,200Mc)
was measured first in a free space pattern range method and
then the measurement was repeated inside the vertical chamber.
To measure the pattern inside the chamber, the antenna was
rotated about a fixed axis and not moved across the chamber.
Therefore, the "available" reflections which exist across the
chamber are not probed and therefore, a rather respectable
pattern can be achieved. As a matter of interest Figure ~~15(b)~~ 13(b)
also shows the effect the wall mount can produce in terms of
reflected energy.
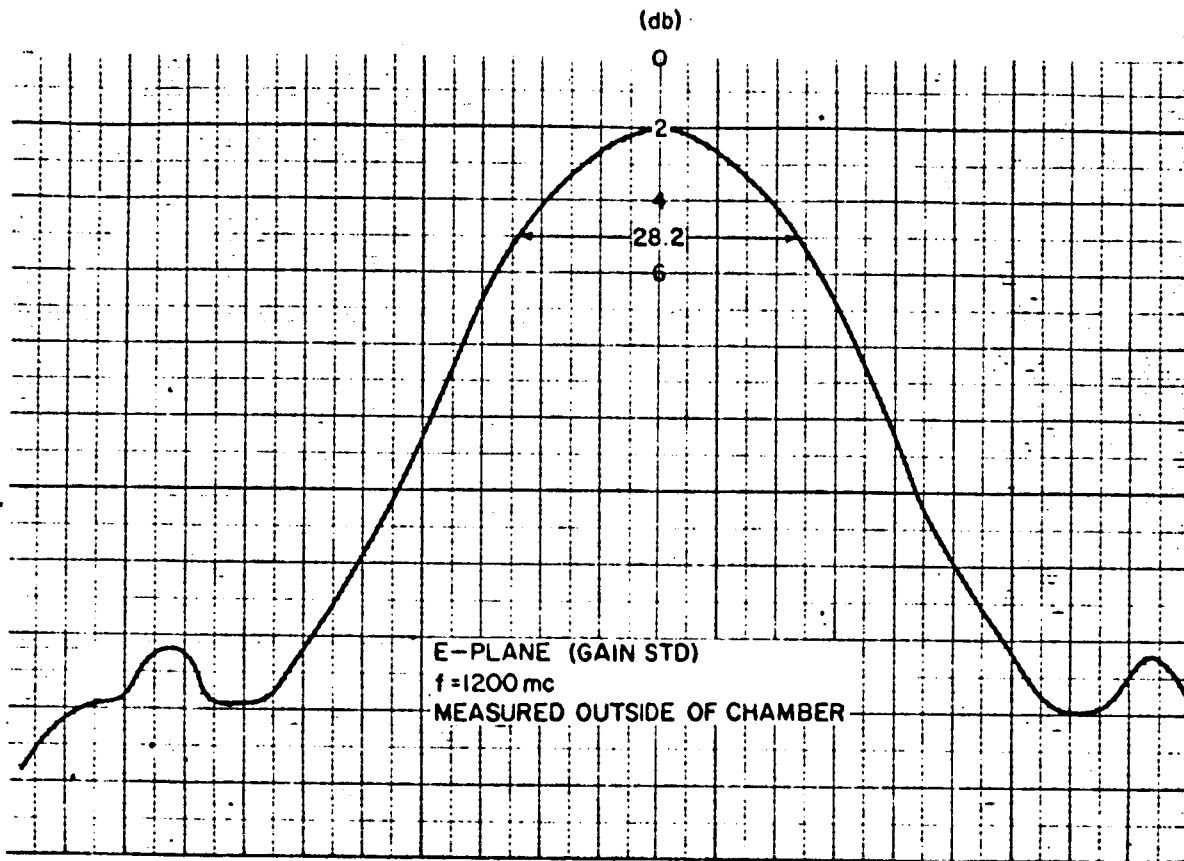
13(a)

Figure ~~13~~ Pattern of Horn Antenna (E-plane) Measured Outside ~~and Inside~~ of Chamber
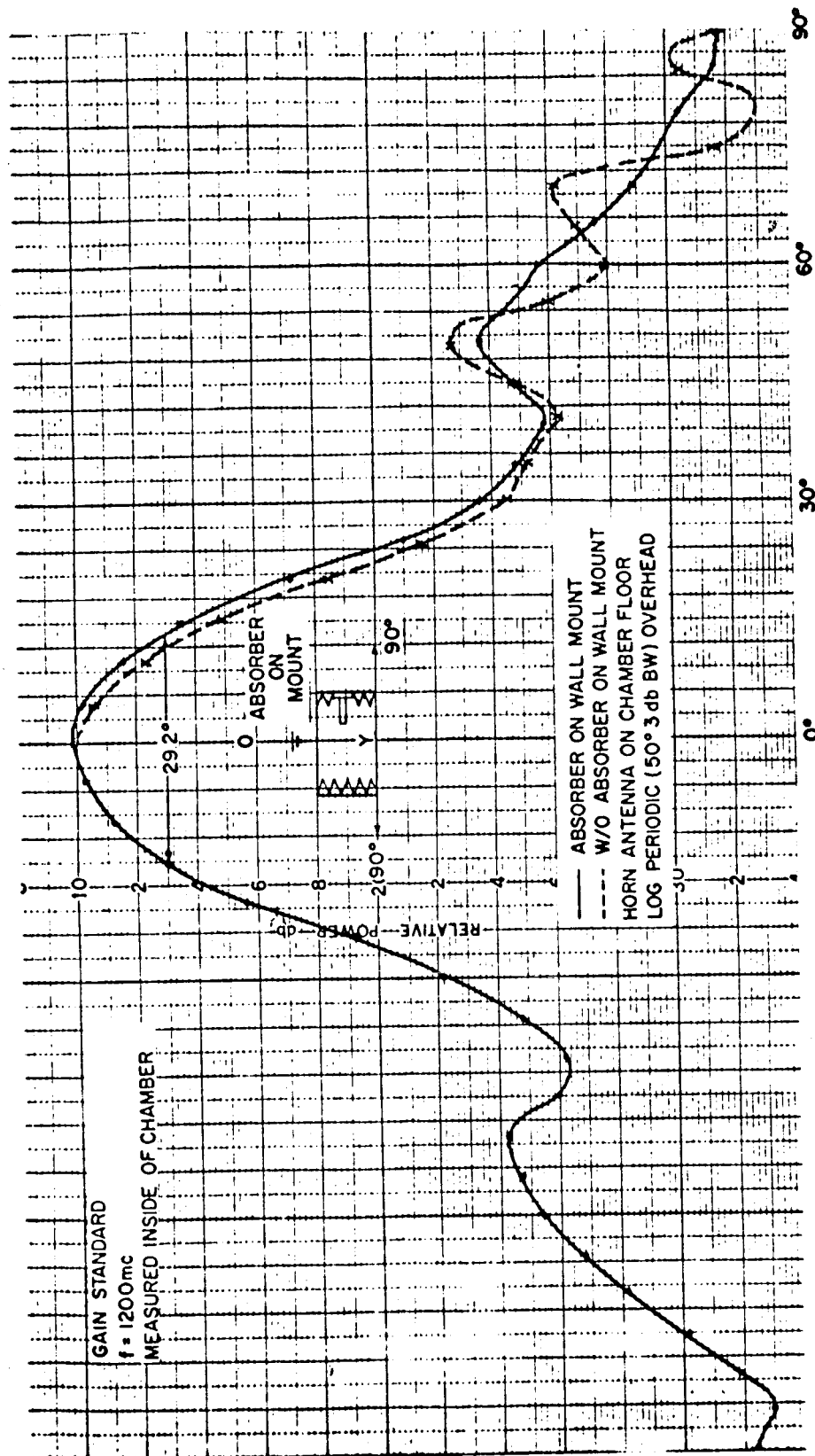
Figure 15. Pattern of Horn Antenna (E-Plane) Measured ~~Outside~~ Inside of Chamber

41

X. Conclusions

Measurements taken from the 1/9th-scale model of the test range are in reasonable agreement with the measurements of the full scale range. The structural A-sandwich radome definitely reduces the performance of the facility at higher frequencies, but does not affect operation in the frequency range of primary interest (125-400Mc).

Considerable confidence may be placed on the results of measuring scale models of anechoic chambers. Since the instrumentation is not difficult and the cost is relatively small it is suggested that more extensive use be made of scale models to check chamber and anechoic material performance.

A multipanel sandwich radome has definite frequency limitations when used as part of an antenna test range. Therefore it is recommended that a thick, low-dielectric-constant foam radome be used.

The concept of a vertical test range composed of an electrically small termination chamber with a r-f transparent radome has been found feasible and provides at moderate cost a convenient, quasi-all-weather, facility for accurate measurement of antenna characteristics.

XI. References

1. Buckley, E. F., "Outline of Evaluation Procedures for Microwave Anechoic Chamber", Microwave Journal, August, 1963.

2. Emerson, W., "Chamber Information", unpublished report of B. F. Goodrich Company.

3. Jasik, "Antenna Engineering Handbook", New York: McGraw-Hill Book Company, 1961.

4. Harvey, "Microwave Engineering", New York, Academic Press, 1963.

5. Electronic Space Structures Corporation, "Ground Radomes", 1964.

43